© 2017. Published by The Company of Biologists Ltd | Journal of Experimental Biology (2017) 220, 4305-4319 doi:10.1242/jeb.164020

RESEARCH ARTICLE

Multimodal *in situ* datalogging quantifies inter-individual variation in thermal experience and persistent origin effects on gaping behavior among intertidal mussels (*Mytilus californianus*)

Luke P. Miller[1,*] and W. Wesley Dowd[2,3]

ABSTRACT

In complex habitats, environmental variation over small spatial scales can equal or exceed larger-scale gradients. This small-scale variation may allow motile organisms to mitigate stressful conditions by choosing benign microhabitats, whereas sessile organisms may rely on other behaviors to cope with environmental stresses in these variable environments. We developed a monitoring system to track body temperature, valve gaping behavior and posture of individual mussels (*Mytilus californianus*) in field conditions in the rocky intertidal zone. Neighboring mussels' body temperatures varied by up to 14°C during low tides. Valve gaping during low tide and postural adjustments, which could theoretically lower body temperature, were not commonly observed. Rather, gaping behavior followed a tidal rhythm at a warm, high intertidal site; this rhythm shifted to a circadian period at a low intertidal site and for mussels continuously submerged in a tidepool. However, individuals within a site varied considerably in time spent gaping when submerged. This behavioral variation could be attributed in part to persistent effects of the mussels' developmental environment. Mussels originating from a wave-protected, warm site gaped more widely, and remained open for longer periods during high tide than mussels from a wave-exposed, cool site. Variation in behavior was modulated further by recent wave heights and body temperatures during the preceding low tide. These large ranges in body temperatures and durations of valve closure events – which coincide with anaerobic metabolism – support the conclusion that individuals experience 'homogeneous' aggregations such as mussel beds in dramatically different fashion, ultimately contributing to physiological variation among neighbors.

KEY WORDS: Biologging, Body temperature, Bivalve, Inter-individual variation, Tidal rhythm, Valve gaping

INTRODUCTION

The extent to which environmental variation affects the performance and survival of organisms can often be mitigated by behavioral strategies that allow organisms to effectively 'smooth' the temporal or spatial variation in the habitat (Angilletta, 2009; Huey et al., 1989; Kearney et al., 2009). These behavioral strategies can work in concert with physiological responses to environmental conditions, and may have important ecological consequences for single species and whole communities, in current and future climate conditions (Harley, 2011; Huey and Tewksbury, 2009; Somero, 2010). The relative importance of physiology and behavior likely depends on the mobility of the species in question (e.g. motile lizards versus sessile intertidal invertebrates) and on the relationship between behavior and parameters (e.g. body temperature, oxygen availability) that directly impinge on physiological performance. However, few data sets exist that have continuously recorded both environmental conditions and behavior of animals in the field at the temporal and spatial resolutions required to resolve these contributions. To address these limitations for the rocky intertidal habitat, we have developed and deployed a custom datalogger system (MusselTracker) that is robust and power-efficient enough to enable long term (multi-week) continuous monitoring of marine mussel temperature and behaviors in wave-swept intertidal conditions.

The wave-swept seashore can be a particularly variable and unpredictable environment owing to the interaction of cycling tides and shifting weather and ocean conditions (Denny et al., 2009). Organism body temperatures, desiccation stress, feeding opportunities and reproductive opportunities may be subject to the timing of short-term and seasonal changes in environmental conditions (Pincebourde et al., 2012). Large-scale latitudinal gradients in variables such as temperature are often matched or exceeded by variation at smaller scales (Helmuth et al., 2006), even at the scale of an organism's body, and coping with this small-scale variation may necessitate that individual organisms have the ability to control or minimize the stress they experience via behavioral means (Chapperon and Seuront, 2011; Hayford et al., 2015; Miller and Denny, 2011; Pincebourde et al., 2016, 2009).

Small-scale variation in environmental conditions such as water flow or solar exposure can be generated by topographic complexity and substratum orientation (Harley, 2008; Helmuth and Denny, 2003; Miller et al., 2009; O'Donnell and Denny, 2008), and foundation species such as mussels can contribute additional microhabitat complexity (Dayton, 1972). Mussel beds are far from homogeneous, and mussels may experience very different water flow, temperature and desiccation conditions (Carrington et al., 2008; Denny, 1995; Helmuth, 1998; Jimenez et al., 2015; Nicastro et al., 2012; O'Donnell, 2008). Effects of environmental variation on mussels can ultimately impact patterns of distribution of many organisms in the intertidal zone via competition or facilitation (Dayton, 1971; Suchanek, 1979).

Previous efforts at monitoring and characterizing variation in rocky shore mussel bed temperatures have used temperature dataloggers attached to the substratum near or inside natural mussel beds (Harley, 2008; Harley and Helmuth, 2003; Petes et al., 2007), or have used mussel mimics containing a temperature data

[1]San Jose State University, Department of Biological Sciences, 1 Washington Square, San Jose, CA 95192, USA. [2]Loyola Marymount University, Department of Biology, 1 LMU Drive, Los Angeles, CA 90045, USA. [3]Washington State University, School of Biological Sciences, PO Box 644236, Pullman, WA 99164, USA.

*Author for correspondence (contact@lukemiller.org)

L.P.M., 0000-0002-2009-6981

Received 31 May 2017; Accepted 23 August 2017

logging device, made using either silicone-filled natural mussel shells or epoxy mimics (Denny et al., 2011; Helmuth et al., 2002; Helmuth and Hofmann, 2001). Measurements of live mussel temperatures have typically been restricted to isolated measurements taken during low tide on a few days with infrared cameras, or via thermistors or thermocouples temporarily inserted into mussels or on the shell surface (Bayne et al., 1976b; Helmuth and Hofmann, 2001; Jimenez et al., 2015; Lathlean et al., 2016). The MusselTracker system bridges this gap between long-term data from biomimetic dataloggers and isolated, short-term live-mussel measurements.

In contrast with body temperature, little is known about the patterns of gaping behavior of mussels living on wave-swept shores. It is not known to what extent individual mussels in an intertidal bed may vary in their time spent gaping or feeding, or whether these behaviors are rigidly driven by the zeitgeber of the tidal cycle. Measurement of bivalve shell gaping has a long history in freshwater and subtidal marine species, primarily under laboratory conditions (Barnes, 1955; Byrne et al., 1990; Dowd and Somero, 2013; Shumway and Cucci, 1987) or in industrial settings where bivalves may be used for monitoring water quality (Sow et al., 2011; Tran et al., 2003). In subtidal field settings, several groups have produced long-duration, high-resolution time series of bivalve shell gaping behaviors, showing evidence of circadian or circalunar rhythms of gape in clams and mussels (García-March et al., 2016, 2008; Schwartzmann et al., 2011), while in tidally influenced channels a tidal rhythm has been observed (Riisgård et al., 2006). Our MusselTracker system may represent the first successful multi-week deployment of a valve gape monitoring system in the wave-swept intertidal zone, where gaping patterns are likely to be driven primarily by tidal cycles, but may also respond to thermal, desiccation and/or hypoxic stress experienced during low tide.

Gaping of the valves during low tide while in air, particularly during high temperature events, has been observed in some species of mussels such as *Perna perna* in southern Africa. The behavior is linked with lower body temperatures compared with closed mussels, presumably owing to the effects of evaporative cooling (Lathlean et al., 2016; Nicastro et al., 2012). However, the invasive species *Mytilus galloprovincialis*, living in the same mussel beds as *P. perna*, was not observed gaping during hot low tides (Lathlean et al., 2016; Nicastro et al., 2012). There is some evidence that the related species *Mytilus edulis* may occasionally gape slightly during aerial emersion (Shick et al., 1986, 1988). Prior laboratory and field studies have noted that *Mytilus californianus* does not readily gape in air at high temperatures (Bayne et al., 1976b; Fitzhenry et al., 2004). We are not aware of any observations of *M. californianus* gaping the shells widely during low tide, and have personally only observed gaping *M. californianus* at low tide that were either already dead or that died shortly thereafter (L.P.M., personal observations). Reports of temperature-related mass mortality events of *Mytilus* species in the field are rare, and these reports do not include direct observations of the mussels' behavior during the heat event (Harley, 2008; Petes et al., 2007; Suchanek, 1978; Tsuchiya, 1983).

Although mussels are nominally sessile as adults, mussel beds are dynamic systems where individuals may move themselves within the mussel matrix. Movement is thought to be driven by the need to achieve a better position for feeding, or to reduce the risk of dislodgement or predation, and could possibly be used to reduce exposure to the sun (Bertness and Grosholz, 1985; de Paoli et al., 2017; Harger, 1968; Robles et al., 2009). Mussels attach themselves to the substratum and to neighbors using flexible byssal threads that degrade over time and can be selectively released by the mussel, but the formation of new threads is energetically costly and is limited at high flow speeds (Carrington et al., 2008). Previous studies have shown that juvenile mussels may be quite mobile within mussel beds, while adult *M. edulis* show little movement (Harger, 1968; Schneider et al., 2005). On wave-swept shores, where the frequent occurrence of high water flows increases the risk of dislodgement to a poorly attached mussel, it is not known how much movement adult *M. californianus* may attempt under natural wave conditions over short time scales of hours to days. We integrated a six-axis accelerometer and magnetometer sensor in the MusselTracker system to enable the first high-resolution tracking of individual mussel movement over these time scales.

The development of a novel and robust biologging system that continuously records body temperature, valve gape and posture allowed us to make a variety of observations and comparisons of mussels at different locations within the wave-swept habitat. In this study, we aimed to characterize the variation in live mussels' body temperatures and thermal stress over both small [a few body lengths within a bed (cm)] and medium spatial scales [between different shore heights (m)]. By simultaneously monitoring both live mussels and biomimetic mussel temperature dataloggers, we explored possible limitations of the biomimetic approach. By monitoring valve gaping, we tested whether mussels differed in the duration and magnitude of valve opening within the same mussel bed and across sites, and how closely valve gape patterns were aligned to tidal or circadian cycles. The combination of temperature and gaping data further allowed us to observe whether *M. californianus* would gape during high temperature events to try to control body temperature via evaporative cooling, or whether conditions experienced during low tide might affect behavior on the subsequent high tide. We tracked body orientation through time to look for evidence that mussels might re-orient themselves to minimize exposure to the sun and thereby moderate body temperature. Finally, we examined whether mussels harvested from two different microhabitats that differ in thermal regime and submersion time might show different behavioral responses to environmental conditions. The multimodal sensor array of the MusselTracker system gives unprecedented insight into the individual experiences of intertidal animals living in a highly heterogeneous environment, laying the technological foundation for *in situ* studies assessing the physiological (e.g. Gleason et al., 2017) and ecological consequences of inter-individual variation in complex habitats.

MATERIALS AND METHODS

Site and collections

The field experiment was carried out at Hopkins Marine Station (HMS), Pacific Grove, CA (36.6217°N, 121.9043°W), on a rocky point that was exposed to northwest swells. We collected adult *M. californianus* Conrad 1837 (n=30, shell length 66.8±3.3 mm, mean ±1 s.d.) from two natural mussel beds: a wave-splashed 'exposed' site and a wave-sheltered 'protected' site where mussels would be splashed less often and would likely be exposed to more frequent high temperature events during their growth. The environmental exposures and corresponding physiological profiles of mussels at these two origin sites have been studied extensively (Denny et al., 2011; Dowd et al., 2013; Jimenez et al., 2015).

The mussels were maintained in a common garden in flowing seawater tables for 7 days prior to the start of the field deployment. Each mussel was measured for length and fitted with a numbered bee tag to identify its origin. The mussels were exposed to a single daily low tide (emersion) while held in the seawater tables, and they

Journal of Experimental Biology (2017) 220, 4305-4319 doi:10.1242/jeb.164020

were fed a commercial feed (Shellfish Diet 1800™, Reed Mariculture, Campbell, CA, USA) once per day.

MusselTracker data acquisition system

One MusselTracker system consisted of a custom-built circuit board holding an ATmega328P microcontroller (Atmel Corporation, San Jose, CA, USA), DS3231 real-time clock (Maxim Integrated, San Jose, CA, USA) and a micro-SD memory card, with ports to attach additional cabled sensors to two mussels (Fig. 1A). A MusselTracker board would operate for approximately 2 weeks on a set of 4 AA batteries. A set of three MusselTracker boards was housed in a watertight box, and two such boxes were attached near the ends of an acrylic plate of dimensions 45×30 cm. Watertight bulkhead fittings allowed sensor wires to be run from the boards to the mussels (Fig. 1B), which were allowed to attach to the acrylic plate between the two boxes. A total of 12 instrumented mussels were mounted on each of the two acrylic plates with two watertight boxes (Fig. 1C). We used a third acrylic plate, for the tidepool location, that only housed one watertight box monitoring six instrumented mussels. All mussels secreted new byssal threads and successfully attached themselves to the plate and their neighbors through the end of the experiment, although three mussels on the high shore plate were consumed by black oystercatchers, *Haematopus bachmani*, during the second and third weeks of the deployment.

Body temperature monitoring

Each MusselTracker monitored the internal body temperature of two *M. californianus* via 30-gauge K-type thermocouples measured with MAX31855K cold-junction compensated thermocouple-to-digital converters (Maxim Integrated). All thermocouples were calibrated in a water bath against an NIST-traceable thermocouple calibrator while attached to their respective MusselTracker boards. For the calibration, the water temperature was raised in 5°C steps from 5°C to 40°C, and linear regressions were fit to each thermocouple against the known water bath temperature in order to apply temperature corrections where needed. Field data from each mussel, sampled every second, were rounded to the nearest 0.25°C – the resolution of the thermocouple convertors – after applying these calibration equations.

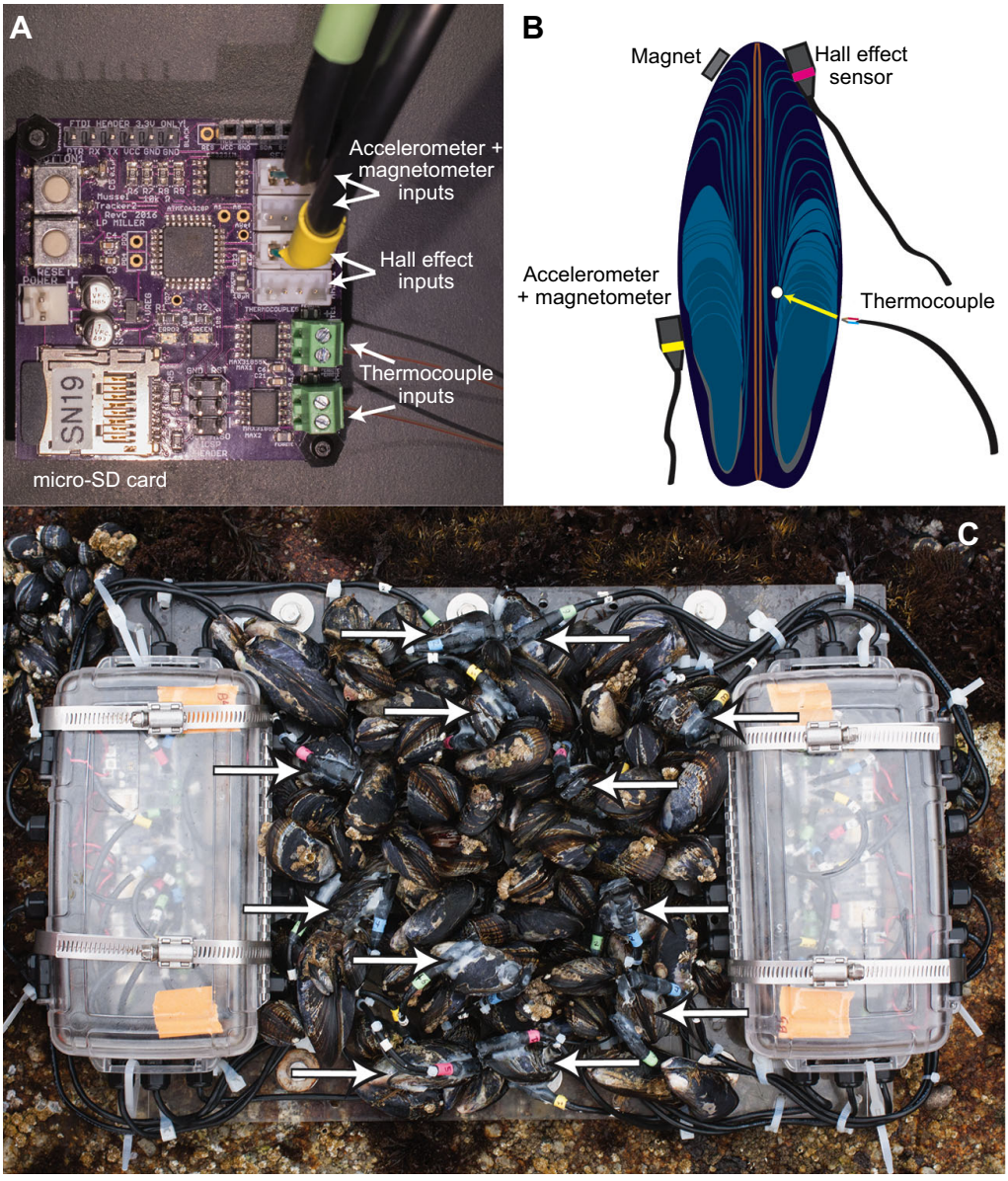

Fig. 1. Illustration of the MusselTracker apparatus. (A) MusselTracker circuit board, containing sensor inputs for two mussels. (B) Diagram of the attachment locations for the sensors on a mussel, ventral view. The thermocouple tip was inserted into a hole drilled in the shell near the ventral margin, as indicated by the arrow. (C) An experimental plate deployed in the intertidal zone. Waterproof boxes on each side hold three MusselTracker boards each, allowing the monitoring of 12 mussels total, indicated by arrows.

To measure mantle cavity temperature (hereafter, body temperature), a 2-mm diameter hole was drilled in the left valve of the mussel, approximately equidistant between the anterior and posterior ends, close to the ventral margin of the valve. This placement ensured that no tissue, other than mantle or gonad, would be impinged upon by the thermocouple. The tip of each thermocouple was coated in polyurethane glue (Amazing Goop, Eclectic Products, Eugene, OR, USA) to prevent water ingress. The coated thermocouple tip was inserted approximately 2–3 mm deep into the hole, where it would rest in contact with the mantle and gonad tissue and be surrounded by mantle cavity seawater. Cyanoacrylate glue was used to seal the hole so that water would not be lost from the mantle cavity during low tide. By the conclusion of the experiment, many mussels had begun to lay down a thin layer of calcium carbonate shell material around the hole at the base of the thermocouple, but we noticed no other adverse responses to the presence of the thermocouple. The temperatures being recorded should be representative of mantle cavity fluid and gonad temperatures, but this method of measurement would not provide information about potential temperature gradients that might exist near the core of the mantle cavity. Temperature data were subset to 10-s intervals for analysis.

Valve gape monitoring

We used Allegro A1393 magnetic Hall effect sensors (Allegro MicroSystems, Worcester, MA, USA) attached via cable to monitor the gape of the shell valves at the posterior end of the mussel. The Hall effect sensor was glued to the left valve of the shell using cyanoacrylate glue and polyurethane cement, while a small magnet was attached directly opposite the Hall effect sensor on the right valve. The Hall effect sensor output a voltage signal that was proportional to the magnetic field strength in its immediate vicinity, so that as the mussel valves gaped, the magnetic field signal became weaker and the voltage signal change was registered by the MusselTracker system. Gape sensor readings were recorded once per second. To avoid the effects of occasional magnetic interference from neighboring mussels that might shift close to the focal mussel, we applied a first-order Butterworth filter to the raw 1 Hz data, and then used the lower 1st percentile and upper 99th percentile values to establish the fully closed and fully open values for the filtered data.

The strength of the magnetic field and resultant voltage signal for each mussel varied according to the precise placement of the Hall effect sensor and magnet on the valves, and the magnetic field strength varied non-linearly with distance as the mussel opened and closed. We fit an asymptotic function using the nlme package in R (Pinheiro and Bates, 2000):

$$\text{Sensor voltage} = a - be^{-c\times\text{Distance}}, \quad (1)$$

to the Hall effect sensor output for a magnet positioned at a set of known distances from a sensor. We used the estimated coefficients to back-calculate valve opening in physical distance (mm) based on Hall effect sensor output. We tested magnets in a variety of starting orientations and distances from the sensor to establish best-fit coefficients for a range of magnet–sensor orientations. A baseline field strength was established when each individual's shell valves were known to be closed. For each mussel, we established the asymptotic 'fully gaped' Hall effect sensor value, represented by the coefficient a in the equation above, using the weakest magnetic signal strength during the time series. The difference between the fully closed and fully open readings from the Hall effect sensor was represented by the coefficient b. The full set of laboratory calibration data for all orientations of the magnet-sensor pair allowed us to calculate a linear regression for coefficient c as a function of $\log(b)$, which we used to then estimate c based on an individual mussel's range of sensor values during the field deployment. After calculating valve gape using the methods above, we converted all values to percent gape – from 0 to 100% of the maximum for each individual – to allow comparison between mussels. In cases where a gape sensor or magnet was dislodged from the mussel, we reattached the sensor or magnet in the field and established a new baseline fully closed value for that mussel in the remaining dataset. The converted gape estimates were analyzed as 1 Hz data for spectral analysis and subset by averaging 10-min intervals to facilitate linear model fitting.

Orientation monitoring

Each mussel was also outfitted with an orientation sensor consisting of a LSM303D combined three-axis accelerometer and three-axis magnetometer (ST Microelectronics, Fairport, NY, USA) attached via cable to the MusselTracker system. The accelerometer and magnetometer allowed the estimation of the mussel's postural orientation (compass heading, pitch and roll) through time. The LSM303D used an internal 50 Hz low-pass filter on the raw data, and was set to record a maximum of ±4 $\boldsymbol{g}$ on the accelerometer and ±8 gauss on the magnetometer. All channels of the LSM303D were recorded at 4 Hz.

The orientation sensor was glued to the right valve, which also held the gape sensor magnet. The orientation sensor was positioned towards the anterior end of the valve, away from the gape sensor magnet. Because the orientation sensor and gape sensor magnet were attached to the same valve, the magnetic field distortion created by the gape sensor magnet should be constant, and thus could be calibrated and compensated for in the compass orientation calculations.

After attaching the orientation sensors, we calibrated them by placing the mussel in a known orientation (horizontal with ventral shell margin pointing down and anterior end pointing north) to establish the orientation of the accelerometer and magnetometer axes relative to the mussel body axes. Each mussel was then slowly rotated through a variety of orientations to establish any offset errors in the accelerometers and to measure scaling and offset errors (also known as 'hard iron' and 'soft iron' effects) in the magnetometer that were induced by the neighboring gape sensor magnet. Scale and offset corrections for both the accelerometer and magnetometer were calculated and applied using functions written in R (R Core Team, 2016), based on the algorithm of Li and Griffiths (2004). Any field measurements where the Euclidean norm of the acceleration vector (x-, y- and z-axes) exceeded 1 $\boldsymbol{g}$±10% were excluded to yield static estimates of orientation without the influence of specific accelerations induced by water motion. For each time point, Euler angles, represented as yaw (heading relative to magnetic north), pitch and roll, were estimated from the accelerometer and magnetometer data following the methods of Ozyagcilar (2012) using functions implemented in R.

Field deployment

Field sites

Prior to the field deployment, the instrumented mussels were held in the seawater table for 2 days and allowed to attach to the acrylic plates with byssal threads. Mussels were arranged on the plates with enough space between individuals to avoid interference from neighboring magnets. Additional 40–70 mm live mussels collected from the field were packed in between the instrumented mussels to create a density similar to a natural mussel bed.

Journal of Experimental Biology

Journal of Experimental Biology (2017) 220, 4305-4319 doi:10.1242/jeb.164020

The plates were deployed to three locations on the wave-exposed point at HMS for 23 days, from the morning of 15 July to the morning of 6 August 2015. The low shore plate was attached to a rock face tilted up 45 deg from horizontal and facing southwest, at a shore height of 1.04 m above mean lower low water (MLLW), immediately adjacent to the 'warm' site illustrated in Dowd et al. (2013). The high shore plate was placed on a horizontal rock face at 1.72 m above MLLW, 4.5 m inshore (southeast) from the low site. The third plate, carrying six instrumented mussels, was mounted in a small tidepool situated 1.45 m above MLLW and 6 m to the southwest of the high site. The tidepool volume was approximately 50 liters, and the instrumented mussels were fully submerged at all times throughout the day, but the tidepool was only filled with new seawater during high tides. The tidepool plate was attached at a 45 deg angle above horizontal, facing west. All shore heights were measured by survey (GTS-211D Total Station, Topcon, Livermore, CA, USA) referenced to a local geodetic benchmark. HMS experiences mixed semidiurnal tides, with one higher high tide followed by a lower high tide on average 12 h 25 min later, along with intervening lower low tide and higher low tide periods. The average diurnal tidal range at HMS is 1.6 m, and the highest tide during the deployment was 1.94 m above MLLW.

We added a plastic mesh cover (5 mm openings) over each plate of mussels prior to deploying them in the field, in order to prevent loss of weakly attached mussels by wave action. The mesh was removed from each plate after 2 days in the field. All plates remained in the field continuously, except for brief 5- to 30-min periods when the plates were detached from the rock to replace batteries.

Environmental data

Air temperature data were obtained from a weather station at HMS situated 30 m south of the field site. Daily sea surface temperature measurements were taken by the HMS caretaker. Air temperature and sea surface temperature were obtained from the Hopkins Marine Life Observatory repository (http://mlo.stanford.edu/). Offshore wave heights were retrieved from a wave rider buoy situated approximately 400 m north of the field site (Coastal Data Information Program buoy 158, Scripps Institute of Oceanography). These data are summarized in Table 1.

Mussel mimic temperature loggers

On day 10 of the field deployment, we added five silicone-filled *M. californianus* shells containing iButton Thermochron temperature data loggers (DS1921G, Maxim Integrated) to the high shore plate. The iButtons were set to record a temperature every 15 min with 0.5°C resolution. The mussel shells were 60–65 mm long, the same size range as the instrumented live mussels. We embedded a plastic cable tie in the silicone and used this to attach the mussel mimic via holes drilled in the plate. The five mussel mimics were deployed haphazardly on the high shore plate in various orientations, immediately next to instrumented live mussels.

Table 1. Environmental conditions at Hopkins Marine Station during the field deployment, 15 July to 6 August 2015

Variable	Overall maximum	Mean±s.d. daily maximum
Solar irradiance (W m^{-2})	1107	914±116
Air temperature (°C)	24.1	19.1±2.0
Sea surface temperature (°C)	21.0	17.1±1.1
Significant wave height (m)	1.46	0.61±0.18

Statistical analyses

All analyses were performed using R 3.3.1 (R Core Team, 2016). In some analyses we included site (high shore, low shore and tidepool) as a fixed factor and treated individual mussels as biological replicates for behavioral or physiological analysis, although the mussels at each of the three locations were grouped closely together on a single experimental plate. The absence of replicate plates for a given shore height limits the generality of shore height comparisons beyond our three sites, but the strong between-site differences observed here are likely representative of the predominant influence of tide cycling and submersion/emersion conditions elsewhere on the shore.

Body temperature analyses

For each mussel, we extracted temperature data for each complete day of the deployment where the mussel was missing no more than 1.5 h of data. The number of mussels on each day that met this requirement varied by day because of sensor failures, dead batteries or mortalities (n=5–12 per day for high and low sites, n=4–6 for tidepool site). We recorded the maximum temperature, T_{max} (°C), and the minimum temperature, T_{min} (°C), for each mussel on each day. The daily maximum heating rate, Q^{+}_{max} (°C h^{-1}), and daily maximum cooling rate, Q^{-}_{max} (°C h^{-1}), for each mussel on each day were both calculated using linear regression in an iterative process. A straight-line regression was fitted to a 45 min window of temperature data to determine the heating or cooling rate. The time window was shifted forward by 5 min and the regression fit repeated, so that a series of heating and cooling rates was calculated for each day, and the extremes were recorded as Q^{+}_{max} and Q^{-}_{max} for that day. We initially calculated heating rates for a variety of time windows ranging from 15 to 75 min, and observed that low tide heating events often had a duration of 45 to 60 min of nearly linear temperature increase before the body temperature began to asymptote, as judged by eye and by R^2 values calculated for the linear fits to different window lengths. We chose a 45 min window as the best compromise in time window sizes that produced realistic, high heating rates without underestimating (via longer windows that included asymptotes) or overestimating heating rates owing to brief temperature jumps (in shorter windows). Cooling events were much more variable in duration, as some occurred entirely in air while others were generated by wave splash and the incoming tide. Cooling often occurred in discrete steps that were likely generated by the initial splash of one or a few large waves, followed by a several-minute period of calm when temperature did not change, and further subsequent temperature decrease as waves hit the site more consistently on the rising tide. Given the variability in cooling patterns, we used the same 45 min window for heating and cooling estimates, and for estimating both rates for the iButton mussel mimics as well.

Several statistics were then estimated from the individual mussel daily temperature metrics to characterize the inter-individual variation in temperatures among mussels situated in the same experimental bed at each of the three sites. The ranges of daily maximum and minimum temperatures among mussels in a site were calculated using the range of T_{max} or T_{min} values for individual mussels at a site within a day, as were the ranges of maximum heating and cooling rates. The means, s.d. and maxima of these ranges were then calculated across the 21 full days of the deployment, leaving out the partial days at the start and end of the deployment. The means of the individual daily metrics (T_{max}, T_{min}, Q^{+}_{max} and Q^{-}_{max}) were calculated for each mussel across all days, and then the mean and s.d. of these per-mussel means were calculated to

estimate the overall average value and variation of each metric within each experimental site.

We estimated the coefficient of variation (CV; the s.d. divided by the mean) for T_{max} and T_{min} following the procedure of Denny et al. (2011), by first subtracting the daily sea surface temperature ($\overline{SST}$) from each estimate of T_{max} and T_{min}. This produces a measure of the variation around a biologically relevant baseline, sea surface temperature, rather than the freezing point of water. The CV_{Tmax} and CV_{Tmin} were calculated for the mussels on each experimental plate each day, after which the mean and s.d. of CV_{Tmax} and CV_{Tmin} for the entire experiment were calculated. The CV of Q^{+}_{max} and Q^{-}_{max} were calculated using the means and s.d. of Q^{+}_{max} and Q^{-}_{max} for the mussels on an experimental plate each day, and then those $CV_{Q^{+}_{max}}$ and $CV_{Q^{-}_{max}}$ estimates for each day were averaged across all days, and the s.d. was calculated.

The cumulative time spent exposed to temperatures that could induce sublethal stress was calculated for the subset of mussels that had temperature data for every day of the experiment (n=6 for the high site, n=7 for the low site, n=6 for the tidepool site). For brief periods during a day where a single mussel may have been missing temperature data (typically because of battery failure), the average temperature of the other mussels on the plate for each time point was used to fill in missing temperature values for the cumulative calculations. A threshold of 25°C was chosen as a temperature beyond which many intertidal molluscs in this central California site begin to exhibit physiological signs of temperature stress (Buckley et al., 2001; Dong et al., 2008; Lockwood et al., 2010; Miller et al., 2009). For each mussel, the cumulative hours spent above 25°C and the degree hours spent above 25°C (body temperature minus 25°C, multiplied by the fraction of an hour of each time step; °H) for the full deployment were tallied.

Comparisons among the three sites of average daily maximum, minimum and overall average temperature, as well as average daily temperature range, were carried out using one-way ANOVA and Tukey HSD *post hoc* tests. Model residuals were visually checked for normality and homogeneity of variance. Comparisons of live mussel and iButton mussel mimic temperature statistics were carried out using *t*-tests.

Valve gape analyses

We defined a gape opening of 20% as the threshold above which we would consider a mussel to be 'open' for the purposes of generating summary statistics on gape behavior, based on the patterns in the empirical cumulative distributions of gape data (Fig. S1) and observations of when water flow became visible from the exhalant siphon of mussels in the laboratory (15–20% gape; L.P.M., personal observations). In other bivalve species, shell gape under an approximate threshold of 20% opening is where siphons may closed enough to end feeding and begin limiting the rate of oxygen exchange with the atmosphere (Ballesta-Artero et al., 2017; Jou et al., 2013). We calculated inter-individual variation statistics for mussels at each experimental site using this 20% gape threshold. We also ran the analyses using thresholds of 10% and 30% to examine the effects of threshold choice. The relative patterns were qualitatively similar, and so we report the results for the 20% threshold only. For each full day of the deployment, we calculated the mean time mussels at a site spent gaped wider than 20%, and the s.d. of the daily time spent gaped wider than 20%. In addition, we report the average across all days of the maximum time any mussel spent gaped wider than 20%. To characterize the differences in time spent gaped widely by mussels sharing the same site, we calculated the maximum, mean, s.d. and CV for the range of time spent gaped on each day. We calculated this range by subtracting the hours spent gaped wider than 20% for the mussel that spent the fewest hours gaped from the mussel that spent the most hours gaping wider than 20%, on each of the 21 full days of the experiment. To examine whether there were individual mussels that consistently spent more time gaping widely compared with other mussels at the same site, we carried out Kruskal–Wallis rank sum tests on the minutes per day spent gaping wider than our 20% threshold. We carried out additional Kruskal–Wallis tests to examine whether mussels from the wave-exposed or wave-protected origins consistently spent more time per day gaping wider than the threshold.

To compare the gaping behavior between mussels at the three experimental sites, and for mussels from the two different origins (wave-exposed site or wave-protected sites), we fit a linear mixed-effects model using experimental site (high shore, low shore, tidepool) and mussel origin (wave-exposed or wave-protected) as predictors, and valve gape as the response. Because the gape data were in the form of proportional values between the limits of 0 and 1, we applied a logit transformation to ensure that the data met the assumption of normality. Gape values at the limits of 0 or 1 were replaced with the smallest non-zero or largest non-one value in the dataset, respectively, prior to transformation. Measurements of gape through time for each mussel were highly correlated, so the model included a first order autoregressive correlation structure (Shumway and Stoffer, 2011). We included a random effect for each individual mussel (i.e. a repeated-measures random effect), based on a significant log-likelihood ratio test of initial models fit with and without the random term (P<0.001). The linear model was initially fit with an interaction between site and origin, but the interaction was non-significant and was dropped from the final analysis, which used the simpler additive model. We subset our original high-frequency (1 Hz) gape data down to averages for 10 min intervals (n=3179 observations per mussel) to reduce the effects of serial autocorrelation. We limited the analysis to mussels that had nearly complete gape data records for the 21 full days of deployment, with no single gap longer than 50 h (n=6 mussels on the high shore plate, n=9 mussels on the low shore plate and n=6 mussels on the tidepool plate). We visually inspected normalized residuals to ensure that the model assumptions of homogeneity of variances and normally distributed residuals in each group were met.

Gape behavior during warm low tide periods was examined by isolating time points where individual mussel body temperatures were above a threshold temperature of 25°C. We calculated median gape opening and range of gape openings during these warm low tides. This analysis only included data from the low shore and high shore experimental plates, where mussels were emersed during low tide, and was carried out on the 10-min subset gape data.

We explored whether higher body temperatures during a low tide were associated with a longer time spent gaping wider than 20% during the subsequent high tide interval (i.e. time from one low tide until the next low tide). Longer periods of gaping might reflect an effort to compensate for a greater oxygen debt or to repair damage incurred during warm conditions, when anaerobic metabolism might increase along with rates of macromolecular damage (Lockwood et al., 2010; Shick et al., 1986). We fit a linear model with wave height and body temperature during the prior low tide as continuous predictors, and field site and origin as categorical predictors. Both wave height and body temperature were standardized (centered and scaled by 1 s.d.) to reduce correlation and facilitate comparison of coefficients. A random effect for individual mussels was included to account for repeated measures of the same mussel across different low tides. Mussels from the tidepool site were excluded from this

Journal of Experimental Biology (2017) 220, 4305-4319 doi:10.1242/jeb.164020

analysis because their maximum body temperatures were low and they had the option to remain open throughout low tide periods in their pool. The model included data for 12 high site and 12 low site mussels, with between three and 41 warm-low-tide observations per mussel, out of a total of 43 low tides during the deployment.

Finally, we used spectral analysis to look for evidence of cyclical patterns in the 1 Hz mussel valve gape data. As with the linear model analysis of gape, we used the subset of the mussels on each plate that contained near-continuous time series with gaps no larger than 50 h. The gaps in each time series were filled via linear interpolation, which permitted the use of longer 530 h time series to provide better frequency resolution at longer periods (time scales of hours to days), at the expense of depressing the relative spectral power at high frequencies (time scales of seconds) (Diggle, 1990; Shumway and Stoffer, 2011). Spectra were smoothed via a Daniell kernel of window width 27 (for the 1 s sample interval) and a 5% taper, using the R package astsa (Stoffer, 2016).

Orientation analyses

To characterize shifts in body position, we restricted our analysis to the total change in orientation between the start and end of the deployment, and to shifts between adjacent low tide intervals. Small changes in orientation occurred at high frequency during high tide, when waves were washing over the experimental plates and mussel valves were opening and closing, but we excluded these time periods from the summary of orientation changes. We excluded data from a small number of mussels that were poorly attached by byssal threads during field observations and mainly anchored by the attached sensor cables. We also had to exclude mussels with failed orientation sensors or insufficient calibration data, yielding results for five mussels on the high shore plate, seven mussels on the low shore plate and six mussels on the tidepool plate. Because mussel exposure to solar irradiance and access to flowing water above the mussel bed should be driven primarily by heading (yaw) and pitch, we considered only these two axes and ignored changes in body roll around the anterior–posterior axis. To summarize changes in orientation, we calculated the combined, absolute change in angle of heading and pitch between each low tide and between the start and end points of the field deployment. Comparisons among sites were carried out using one-way ANOVA.

RESULTS

Body temperature

Variation in daily maxima and minima among sites and individuals

Summary statistics and comparisons of daily temperature maxima, minima, means, heating rates and cooling rates are provided in Table 2 and the Appendix. Among the three field locations, mussels at the high shore site consistently experienced the greatest magnitude of inter-individual variation in body temperature (Figs 2 and 3). Specifically, the high site exhibited the greatest mean range in individuals' daily maximum temperatures (7.0°C) as well as the highest overall maximum range of daily T_{max} among individuals (14.2°C). Therefore, even on some of the warmest days, some mussels at the high site experienced body temperatures below the level that would induce cellular stress (Fig. 3). The average daily maximum temperatures among mussels on the high plate were significantly different ($F_{5,120}$=6.24, P<0.001, n=6 mussels with complete 21-day temperature records). Overall, these results confirm that live mussels only a few body lengths apart can reach very different peak temperatures on the same day within the same mussel bed. Notably, the s.d. of the daily range of T_{max} over the course of the experiment was greatest at the low-shore site (4.29°C),

Table 2. Inter-individual temperature variation and temperature change rate statistics for mussels from each of the three field sites

Variable (units)	High shore	Low shore	Tidepool
Overall maximum temperature T_{max} (°C)	38.5	33.8	26.2
Mean range of T_{max} (°C)	7.0	4.5	1.8
s.d. of range of T_{max} (°C)	2.58	4.29	0.78
Maximum range of T_{max} (°C)	14.2	12.8	3.0
Mean individual T_{max} (°C)	25.8	19.8	20.8
Mean s.d. of individual T_{max} (°C)	3.54	2.62	1.41
Mean CV of T_{max}–$\overline{SST}$	0.27	2.25	0.17
s.d. of CV of T_{max}–$\overline{SST}$	0.10	9.77	0.16
Overall minimum temperature T_{min} (°C)	11.8	12.2	13.0
Mean range of T_{min} (°C)	0.94	1.3	0.32
s.d. of range of T_{min} (°C)	0.25	0.61	0.12
Maximum range of T_{min} (°C)	1.5	2.75	0.5
Mean individual T_{min} (°C)	13.9	15.0	15.2
Mean s.d. of individual T_{min} (°C)	0.95	1.1	1.0
Mean CV of T_{min}–$\overline{SST}$	−0.13	0.01	−0.13
s.d. of CV of T_{min}–$\overline{SST}$	0.07	0.86	0.13
Overall maximum heating rate Q^{+}_{max} (°C h^{-1})	20.2	12.4	4.2
Mean range of Q^{+}_{max} (°C h^{-1})	5.4	1.8	0.34
s.d. of range of Q^{+}_{max} (°C h^{-1})	4.15	2.58	0.73
Maximum range of Q^{+}_{max} (°C h^{-1})	14.7	10.8	2.3
Mean individual daily Q^{+}_{max} (°C h^{-1})	6.79	1.32	0.50
Mean s.d. of individual daily Q^{+}_{max} (°C h^{-1})	3.84	1.26	1.08
Mean CV of Q^{+}_{max}	0.26	0.42	0.27
s.d. of CV of Q^{+}_{max}	0.12	0.30	0.03
Overall maximum cooling rate Q^{-}_{max} (°C h^{-1})	−22.8	−16.8	−5.31
Mean range of Q^{-}_{max} (°C h^{-1})	6.2	2.4	0.36
s.d. of range of Q^{-}_{max} (°C h^{-1})	3.10	3.99	0.87
Maximum range of Q^{-}_{max} (°C h^{-1})	13.5	16.0	3.0
Mean individual daily Q^{-}_{max} (°C h^{-1})	−7.9	−1.3	−0.7
Mean s.d. of individual daily Q^{-}_{max} (°C h^{-1})	3.85	1.53	1.49
Mean CV of Q^{-}_{max}	−0.29	−0.47	−0.20
s.d. of CV of Q^{-}_{max}	0.13	0.37	0.12

T_{max}, maximum temperature; T_{min}, minimum temperature; $\overline{SST}$, daily sea surface temperature; Q^{+}_{max}, daily maximum heating rate; Q^{-}_{max}, daily maximum cooling rate.

The overall maximum and minimum temperatures represent the single warmest or coldest mussel at each site during the entire experiment. Overall measures of Q^{+}_{max} and Q^{-}_{max} represent the single fastest warming or cooling event across all of the mussels at a site during the deployment. For the other metrics, T_{max}, T_{min}, Q^{+}_{max} or Q^{-}_{max} was recorded for each available mussel on a given day to generate estimates of the metric within each site on each day, and summary statistics were then calculated across all 21 full days of the field deployment. Samples sizes on each day ranged from 5 to 12 for the high shore site (mean=8 mussels per day), 5 to 12 at the low shore site (mean=10.8 mussels per day) and 4–6 at the tidepool site (mean=5.7 mussels per day).

reflecting occasional instances when calm sea conditions and late afternoon sun combined to heat up mussels at the upper edge of the plate that had not yet been submerged by the incoming high tide. This day-to-day fluctuation in the magnitude of temperature variation among mussels at the low-shore site also led to a greater mean (2.25) and s.d. (9.77) for the CV in $T_{max} - \overline{SST}$ compared with the high shore and tidepool sites, which were more consistent across days in their magnitudes of within-site variation.

Within-site variation in the daily minimum mussel body temperatures, which were generally achieved at night, showed reduced magnitudes (mean range=0.32–1.3°C) as well as more consistency (s.d. of ranges=0.12–0.25°C) across the three sites than did daily maximum temperatures (Table 2).

Inter-individual variation in cumulative thermal stress

Among the subset of mussels that had functional temperature sensors for the entire field deployment, high site mussels spent an

Journal of Experimental Biology (2017) 220, 4305-4319 doi:10.1242/jeb.164020

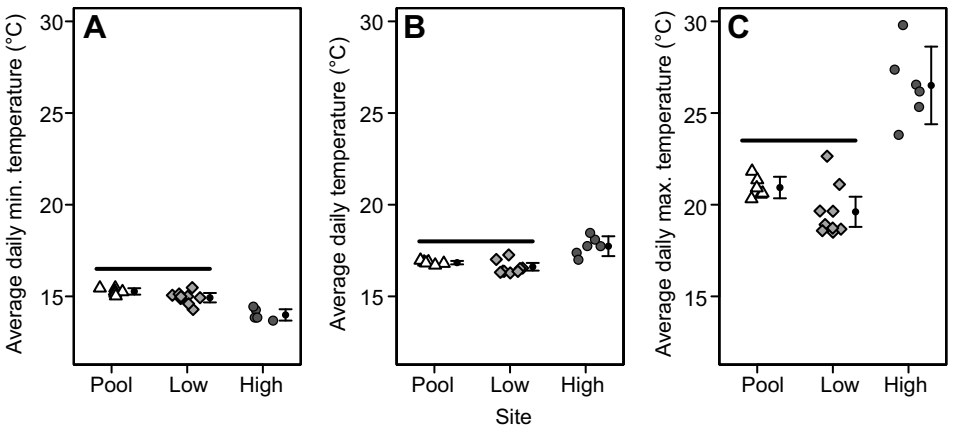

Fig. 2. Average daily temperatures for the three field locations. (A) Average daily minimum temperature; (B) average daily temperature; (C) average daily maximum temperature. Black points and error bars represent the mean and 95% CI for each location, while white triangles, gray diamonds and gray circles represent individual mussel values. Averages were calculated using the six to seven mussels per plate that survived for the entire 21 full days of the field deployment. For each temperature metric, black bars over pairs of sites indicate mean temperatures that were not significantly different based on Tukey's HSD *post hoc* comparisons.

average of 30.7±12.6 (all values ±1 s.d. hereafter unless otherwise specified) hours at temperatures above 25°C, while mussels at the low shore and tidepool sites spent considerably less time at temperatures above that threshold (2.35±3.9 and 0.07±0.2 h, respectively, Fig. S2A). The degree hours above 25°C (°H) were also much higher on average for the high site (85±62.9°H, Fig. S2B) relative to the other sites, reflecting the fact that mussels were not only spending more time above the threshold, but also achieving higher maximum temperatures.

Live versus mimic mussels

Silicone-filled mussel mimics containing iButton temperature dataloggers performed similarly to the live mussels on the high shore plate (Table 3). For the 11 days when both live mussels and iButton mimics were present on the high shore site, there were no significant differences in average daily minimum temperatures (Welch's two-sample *t*-test, $t_9=-1$, $P=0.2$; Fig. 4A), average daily temperature ($t_8=-1$, $P=0.2$; Fig. 4B) or average daily maximum temperature ($t_6=-0.1$, $P=0.9$; Fig. 4C). The daily average range of temperatures experienced during the 11 days by live and mimic mussels were nearly equal, 13.6±3.87°C for live mussels and 13.5±4.08°C for mimics. Although the average daily maxima for the two groups overlapped, when individual live mussels were compared with their nearest iButton mimic neighbor (either in direct contact or less than 1 cm away), the absolute difference in daily maximum temperature for each pair was on average 2.9±0.64°C ($t_{48}=9.4$, $P<0.001$).

Mean heating rates were approximately 1°C h^{-1} faster for live mussels (7.1±3.73, overall maximum 19.2°C h^{-1}) than for mimics (6.1±3.95°C h^{-1}, overall maximum 18.8°C h^{-1}), and live mussels cooled off slightly faster than mimics on average (mean $Q^{-}_{max}=-9.0\pm5.43$ and -8.2 ± 5.26°C h^{-1}, respectively). For both heating and cooling, live mussels heated at rates that were more similar to each other (mean range of $Q^{+}_{max}=3.8\pm3.1$°C h^{-1}) compared with the neighboring mimic mussels (mean range of $Q^{+}_{max}=5.2\pm3.4$°C h^{-1}).

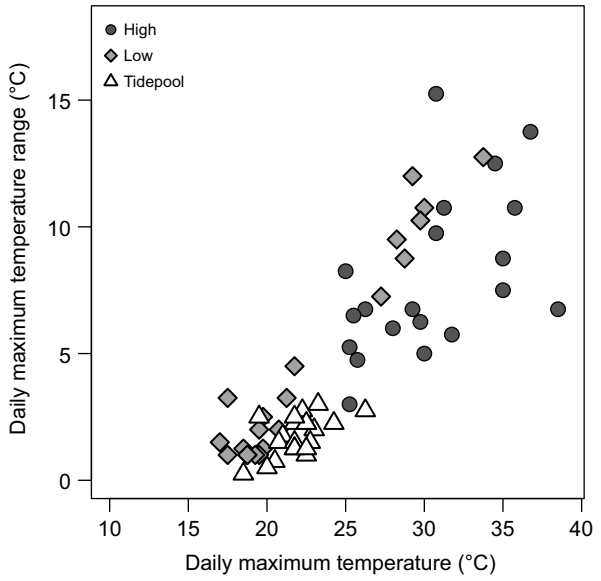

Fig. 3. Correlation between the overall maximum mussel body temperature on a given day and the range of mussel maximum body temperatures at the same site on that same day. Correlation coefficients are: high site $r=0.56$, low site $r=0.97$, tidepool site $r=0.58$, and for all sites pooled $r=0.85$ ($P<0.01$ for each correlation).

Gaping behavior

Inter-individual variation in percentage of time spent gaping

The time per day spent gaping wider than the 20% threshold differed between the high shore site and the other two sites (Table 4, Fig. S1), with the high shore site mussels spending approximately one-third as many hours per day gaping. The variation among adjacent mussels in mean hours per day spent gaped was also lowest at the high shore site (s.d.=1.2 h day^{-1}) compared with the low shore mussels (2.8 h day^{-1}) and the tidepool mussels (3.1 h day^{-1}). When expressing gape behavior as the range in values between the mussel spending the most hours per day and the mussel spending the fewest hours per day gaped wider than 20%, the high shore site mussels had a smaller maximum range (6.2 h) compared with the low shore and tidepool sites, where both ranges exceeded 14 h. The mean daily range among mussels of time spent gaped was lower for the high shore site (3 h day^{-1}) compared with the other two sites (8 h day^{-1}). Among the mussels at each site, there were individuals that consistently spent more time per day gaped wider than the 20% threshold compared with their neighbors (Kruskal–Wallis rank sum test, $\chi^2_5=20.6$, $P<0.001$ at the high shore site, $\chi^2_8=44.4$, $P<0.001$ at the low shore site, and $\chi^2_5=35.6$, $P<0.001$ at the tidepool site).

Persistent effects of origin site on overall mean gape

Empirical probability density distributions indicated that mussels at the high shore site spent much less of their time with the valves gaped widely, while the mussels on the low shore and tidepool plates had similar distributions to each other (Fig. 5). The linear model of logit-transformed valve gape versus experimental site and mussel origin (wave-exposed or wave-protected origin) indicated both factors were predictive (intercept, $\chi^2_1=1169.1$, $P<0.0001$;

Journal of Experimental Biology (2017) 220, 4305-4319 doi:10.1242/jeb.164020

Table 3. Inter-individual temperature variation and temperature change rate statistics for live mussels and silicone-filled mussel mimics containing an iButton temperature datalogger deployed at the high shore site

Variable (units)	Live mussels	Silicone-filled mussel mimics
Overall maximum temperature T_{max} (°C)	38.5	41.5
Mean range of T_{max} (°C)	5.8	9.0
s.d. of range of T_{max} (°C)	1.59	2.48
Maximum range of T_{max} (°C)	8.8	12.5
Mean individual T_{max} (°C)	27.4	27.6
Mean s.d. of individual T_{max} (°C)	3.82	4.17
Mean CV of T_{max}–$\overline{SST}$	0.2	0.3
s.d. of CV of T_{max}–$\overline{SST}$	0.06	0.09
Overall minimum temperature T_{min} (°C)	12.0	12.0
Mean range of T_{min} (°C)	0.9	1.1
s.d. of range of T_{min} (°C)	0.28	0.91
Maximum range of T_{min} (°C)	1.5	3.5
Mean individual T_{min} (°C)	13.7	14.1
Mean s.d. of individual T_{min} (°C)	0.89	0.94
Mean CV of T_{min}–$\overline{SST}$	−0.2	−0.3
s.d. of CV of T_{min}–$\overline{SST}$	0.08	0.14
Overall maximum heating rate Q^{+}_{max} (°C h^{-1})	19.2	18.8
Mean range of Q^{+}_{max} (°C h^{-1})	3.8	5.2
s.d. of range of Q^{+}_{max} (°C h^{-1})	3.09	3.40
Maximum range of Q^{+}_{max} (°C h^{-1})	11.3	11.6
Mean individual daily Q^{+}_{max} (°C h^{-1})	7.1	6.1
Mean s.d. of individual daily Q^{+}_{max} (°C h^{-1})	3.73	3.95
Mean CV of Q^{+}_{max}	0.2	0.4
s.d. of CV of Q^{+}_{max}	0.07	0.15
Overall maximum cooling rate Q^{-}_{max} (°C h^{-1})	−22.8	−24.8
Mean range of Q^{-}_{max} (°C h^{-1})	5.4	6.4
s.d. of range of Q^{-}_{max} (°C h^{-1})	3.13	4.16
Maximum range of Q^{-}_{max} (°C h^{-1})	13.1	14.2
Mean individual daily Q^{-}_{max} (°C h^{-1})	−9.0	−8.2
Mean s.d. of individual daily Q^{-}_{max} (°C h^{-1})	5.43	5.26
Mean CV of Q^{-}_{max}	−0.3	−0.3
s.d. of CV of Q^{-}_{max}	0.13	0.17

The overall maximum and minimum temperatures represent the single warmest or coldest mussel or mimic during the 11 full days of the mussel mimic deployment. Overall measures of Q^{+}_{max} and Q^{-}_{max} represent the single fastest warming or cooling event across all of the live mussels or mimics during the 11 full days of the mussel mimic deployment. For the other metrics, T_{max}, T_{min}, Q^{+}_{max} or Q^{-}_{max} was recorded for each of six live mussels or five mimics on a given day to generate estimates of the metric on each day, and summary statistics were then calculated across all 11 full days.

origin, $\chi^2_1 = 7.8$, P=0.005; site, $\chi^2_2 = 146.8$, P<0.0001; parameter estimates provided in Table S1). Individual mussels on the low shore and tidepool plates did not differ significantly in their average gape opening [−1.63±0.13 among tidepool mussels and −1.81±0.10 for the low shore site mussels (least-squares means±1 s.e.m., logit-transformed valve gape percentage), Tukey's HSD P=0.5], but mussels on the high shore had significantly narrower average valve gape over the duration of the field deployment compared with the low shore and tidepool sites [high shore least-squares mean −3.54± 0.13 (±1 s.e.m., logit-transformed), Tukey's HSD P<0.0001 for comparisons to low shore and tidepool site mussels]. Across all three experimental sites and all time points, mussels originating from the wave-protected site tended to open their valves more widely compared with mussels originating from the wave-exposed location, though the absolute difference between mussels of the two different origins was generally small at all three sites (1–5% wider opening of wave-protected origin mussels on average, based on back-transformed least squares means). The comparison of mean ranks for time per day spent gaped wider than 20% indicated that wave-protected origin mussels spent more time open than mussels from the wave-exposed origin site, at all three experimental sites (Kruskal–Wallis rank sum test, high site, $\chi^2_1 = 15.9$, P<0.001; low site, $\chi^2_1 = 7.34$, P=0.007; tidepool site, $\chi^2_1 = 9.78$, P=0.002).

Variation in behavior during warm low tides and subsequent high tides

Mussels experiencing high body temperatures (>25°C) during low tide aerial emersion generally kept their valves closed (range of median gape openings 0.2–5%, overall median 1.4%), and the widest gape observed during any single warm low tide period was 12.2%.

Mussel gaping behavior during high tide showed a series of interactions with offshore wave height, shore location, mussel origin and maximum body temperature during the prior low tide (Table S2, Fig. S3). Increasing wave heights had a significant, positive effect on time spent gaping wider than 20% during a high tide interval (analysis of deviance, $\chi^2_1 = 259.2$, P<0.001). Mussels placed at the low site gaped for longer periods ($\chi^2_1 = 149.4$, P<0.001), and the low-shore mussels exhibited the greatest dependence of gaping behavior on prior wave conditions (wave height×site interaction, $\chi^2_1 = 33.6$, P<0.001). Across all sites, mussels gaped for marginally shorter periods when they had reached a higher maximum body temperature (main effect of temperature, $\chi^2_1 = 4.7$, P=0.03), while temperature and wave height had a significant interaction (temperature×wave height, $\chi^2_1 = 14.2$, P<0.001), with increases in both factors tending to increase time spent gaping during high tide. Mussels originating from the wave-protected site gaped more than those from the wave-exposed site ($\chi^2_1 = 5.5$, P=0.019). There was also a marginally significant interaction between prior maximum body temperature and mussel origin (temperature×origin interaction, $\chi^2_1 = 4.7$, P=0.03),

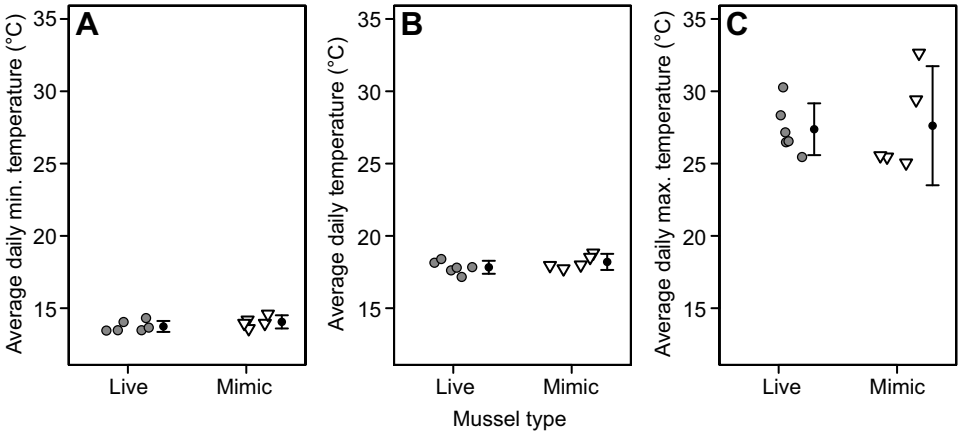

Fig. 4. Average daily temperatures for live mussels (gray circles) or mussel mimics (white triangles) containing iButton temperature dataloggers attached on the high shore plate. (A) Average daily minimum temperature; (B) average daily temperature; (C) average daily maximum temperature. Black points and error bars represent the mean and 95% CI for each type. Live mussel data only includes mussels that were present for all 11 full days that the mussel mimics were attached (n=6 live, n=5 mimics).

Journal of Experimental Biology (2017) 220, 4305-4319 doi:10.1242/jeb.164020

Table 4. Inter-individual variation in time per day spent gaped wider than a threshold value of 20%, for mussels at each of the three field sites

Variable (units)	High shore	Low shore	Tidepool
Mean maximum time gaped>20% (h day^{-1})	6.0	18.1	18.5
Mean time gaped>20% (h day^{-1})	4.4	14.4	14.7
Mean s.d. of time gaped>20% (h day^{-1})	1.21	2.87	3.17
Maximum range of time gaped>20% (h day^{-1})	6.2	14.1	14.8
Mean range of time gaped>20% (h day^{-1})	3.1	8.1	8.2
Mean s.d. of range of time gaped>20% (h day^{-1})	1.6	3.1	3.1
CV of range of time gaped>20%	0.54	0.39	0.38

Each metric was calculated for each full day in the field deployment, and mean values were calculated by averaging the results for all 21 days in the dataset, while the maximum range of time gaped>20% represents the overall maximum among all days. Sample sizes were n=6 for the high shore site, n=9 for the low shore site and n=6 for the tidepool site.

with mussels originating from the wave-exposed site showing a small decrease in time spent gaping on warmer days relative to the wave-protected origin mussels.

Circadian versus circadian rhythms

Spectra derived from the time series of the mussel gape sensors revealed the largest peak in gape change at a period length of 12 h 25 min (Fig. 6). This period aligns with a half-cycle of the circadian cycle (24 h 50 min) and should represent peaks in gape change associated with the two daily high tide periods. The high shore mussels showed a secondary peak in the spectra close to the full circadian period. However, the low shore and tidepool mussels, which spent far more of their time submerged relative to the high shore mussels, exhibited a shift in the secondary spectrum peak closer to a 24 h period, perhaps reflecting changes in gape behavior associated with day versus night rather than being tied to the timing of the second high tide each day. There was no signature of large variation in valve gape spectra at shorter time periods, indicating no consistent cycling of the valves open and closed on time scales of seconds to minutes (data not shown).

Orientation

Between the start and end of the deployment period, mussels shifted their orientation (absolute combined change in heading and pitch) an average of 30±20.5 deg (range 2 to 71 deg), and there were no significant differences in movement among the three sites ($F_{2,19}$=0.69, P=0.51). There was no correlation between orientation change during the deployment and average daily maximum temperature (P=0.4) or °H above 25°C (P=0.5). The orientation change between subsequent low tide periods averaged 7±7.7 deg, but with a greater range in orientation shifts (range 0 to 96 deg) compared with the start and end points of the deployment. A one-way ANOVA indicated a small difference in tide-to-tide orientation change ($F_{2,562}$=4.96, P<0.007) between sites, with the tidepool mussels moving less than the high shore or low shore mussels (Tukey's HSD, low shore versus tidepool, P=0.03; high shore versus tidepool, P=0.01). However, the magnitude of the differences between sites was small (least squares means: 8.1 deg high plate, 7.6 deg low plate, 5.5 deg tidepool).

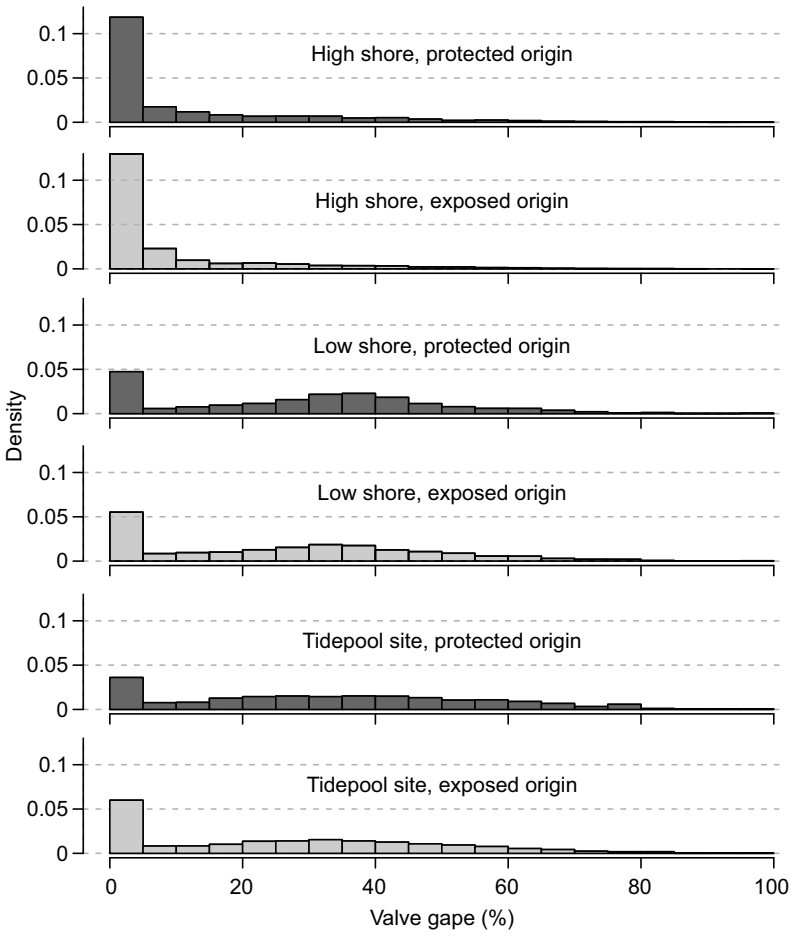

Fig. 5. Empirical probability density distributions of valve gape opening (%) at the three experimental locations (high shore, low shore and tidepool), separated based on the origin of the mussels. Mussels were originally harvested either from a wave-protected or wave-exposed site. The number of focal mussels in each group are n=3, 4, 4, 5, 3 and 3, respectively, for each panel from top to bottom. Densities were normalized so that the area under all distributions=1.

Journal of Experimental Biology

Journal of Experimental Biology (2017) 220, 4305-4319 doi:10.1242/jeb.164020

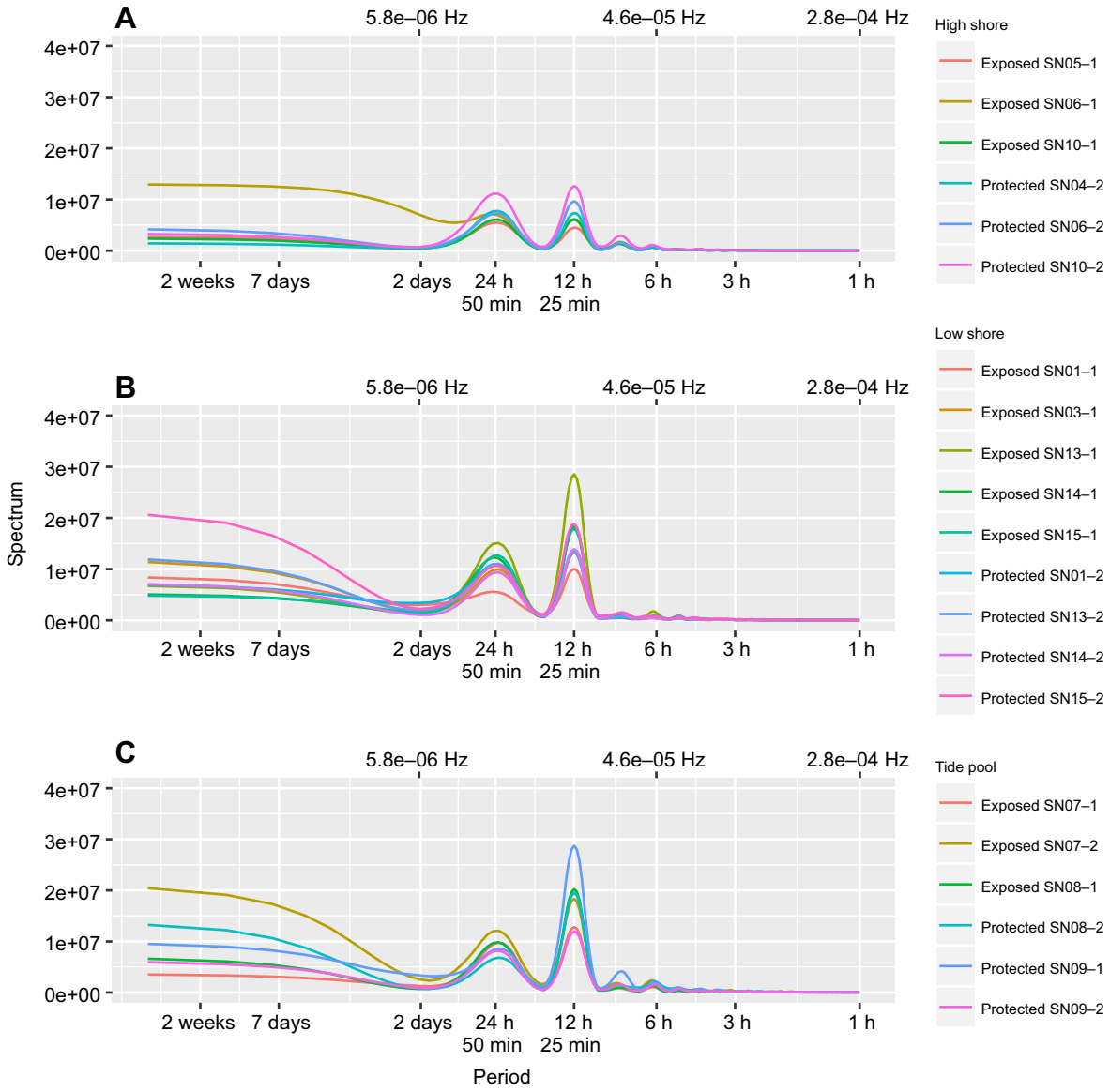

Fig. 6. Smoothed spectral estimates for shell gape behavior of mussels at the three sites. (A) High shore; (B) low shore; (C) tidepool. Units on the ordinate axis are (proportional gape opening)^2 Hz^{-1}. Colored lines represent individual mussels that were originally collected from the wave-exposed or wave-protected field site. Only data from mussels with nearly continuous time series were included in the analysis (n=6 to 9 per site). There were no large peaks at time periods shorter than 1 h, so the plots have been truncated to improve the clarity of longer period patterns. The main peak in each panel falls closest to 12 h 25 min (half of a 24 h 50 min circatidal period) rather than a 12 h diel harmonic. For the high shore mussels, the secondary peak falls close to the circatidal period at 24 h 50 min, but the low shore and tidepool mussel secondary peaks are primarily centered near the 24 h period.

DISCUSSION

Individual biologging of intertidal mussels confirmed persistent differences in thermal experience among neighboring mussels, while revealing origin effects and environmental influences on gaping behavior. Our continuous measurements of *M. californianus* internal body temperature, valve gape and body orientation in a wave-swept intertidal field site reinforce and extend existing hypotheses on how small-scale environmental heterogeneity may impact feeding, growth and survival of this habitat-forming species that is a dominant competitor for primary space (Dayton, 1971; Paine, 1974; Suchanek, 1981). Attempts to quantify the range in inter-individual variability in behavior or physiology necessarily require large samples sizes and/or long-term monitoring to capture the true range of variability. With the MusselTracker system, we have made relatively long-term (21 day) observations that begin to capture the potential range of this variability, but larger sample sizes and longer deployments would further clarify patterns of variation among mussels within and between mussel beds on the shore. Our studies were conducted in summer, when waves are relatively small along the California coast. There may be less variation among individuals in body temperature and/or behavior during fall and winter, when larger waves are common.

Micro-scale variation in maximum body temperatures and cumulative thermal stress

Key among these multi-week observations is confirmation that the range in body temperatures experienced by live mussels at spatial scales of a few body lengths can equal or exceed the mean variation in body temperatures at latitudinal scales (Denny et al., 2011; Helmuth et al., 2016, 2002). Whereas Denny et al. (2011) observed

Journal of Experimental Biology (2017) 220, 4305-4319 doi:10.1242/jeb.164020

inter-individual variation in daily maximum temperatures among biomimetic dataloggers of 3.7 to 6.4°C (maximum range of 15.2°C), we observed a larger average range of 7.0°C and a similar maximum range of 14.2°C within a single day for live mussels at our high shore site, located only a few meters from the Denny et al. mussel bed. We also confirmed previous observations that inter-individual variation in maximum daily body temperature increases as the mean temperature increases (i.e. body temperature follows a heteroscedastic pattern). This small-scale variation in individual mussel thermal experiences was reflected in the large differences in the cumulative time spent at temperatures above 25°C during the 3-week deployment (e.g. range of 52.6 to 16.3 h for mussels within the high shore plate), and it could lead to dramatically different physiological stress profiles for mussels living within the same bed (Gleason et al., 2017). In contrast, individuals experienced consistent daily minimum temperatures, regardless of intertidal position or location within a mussel bed. Whether this latter observation extends to extreme cold conditions in colder seasons or higher latitudes remains to be determined.

Our results indicate that, for certain applications, nearby biomimetic temperature dataloggers can be reasonable proxies for *in situ* live mussel internal temperatures at all phases of the tidal cycle. Biomimetic mussels deployed on our high shore plate demonstrated similar daily minimum, average and maximum temperatures to instrumented live mussels; heating rates during low tide were comparable as well. It clearly remains necessary to use several dataloggers spread through mussel beds to account for the myriad small-scale effects of site slope, azimuth, wave exposure and neighbor shading that can affect the rate of heating and cooling of biomimetic dataloggers, but when appropriately deployed, these tools can provide an accurate picture of mussel bed thermal characteristics over long time scales (Helmuth et al., 2016). However, caution should be exercised in extrapolating from the temperature data of one or a few mimics to the thermal experience of individual live mussels in the same bed. Efforts to quantify environmental effects on an individual's level of stress, as opposed to mean differences (such as those between sites), would arguably be better served by utilizing the individual biologging approach demonstrated here, or by focusing the collection of individuals for physiological sampling on mussels that are in immediate contact with mimic mussels that share the same size and position in the mussel bed. For example, we have carried out biochemical assays of oxidative damage on the same sets of mussels monitored in the current project, and found that inter-individual variation in thermal experience and, to a lesser extent, behavior, correlates to a significant degree with inter-individual variation in biochemical profiles (Gleason et al., 2017).

Achieving extreme high temperatures during low tide on rocky shores requires a confluence of specific environmental conditions (e.g. calm waves, calm winds, daytime low tide, high irradiance) that may only happen at certain times of the year (Denny et al., 2009). The high heating rates we observed indicate that these factors need not coalesce for long; mussels can reach extreme, physiologically stressful temperatures in less than an hour under the right conditions. The maximum heating rates observed at our high shore and low shore sites (20.2 and 12.4°C h^{-1}, respectively) were substantially higher than those reported by Denny et al. (2011) for silicone-filled mussel mimics (5.6 to 8.1°C h^{-1}) deployed a few meters from our study location in wave-protected natural mussel beds at HMS. Denny et al. (2011) did not report mean daily maximum heating rates, but at our high shore site this rate was 6.8°C h^{-1}, within the range of overall maxima they reported. These differences between studies may be due in part to differing environmental conditions during the summers of the respective experiments, as our average daily maximum air temperature was over 3°C warmer and average sea surface temperature was 2.6°C warmer than the 2010 conditions reported in Denny et al. (2011). In particular, the warmer air temperatures during our study should have allowed mussel body temperatures to reach higher values before convective heat loss to the air offset additional heat gain from solar irradiance (Helmuth, 1998).

Variation in gaping behavior

Superimposed on this inter-individual variation in body temperature was a surprisingly substantial amount of inter-individual variation within sites in time spent with the valves gaping open while submerged or splashed during high tide. This implies large differences among neighboring mussels in time for access to food and oxygen, as well as the opportunity to excrete wastes, all of which could impact long-term performance metrics such as growth rates (Bayne et al., 1976a,b). At all three locations, there were individual mussels that consistently spent more time gaping widely each day compared with their neighbors, even among mussels continuously submerged in the tidepool. Similar individual consistency in the extent of gaping through time has been observed in *M. edulis* (Shick et al., 1986). Persistence of this behavior in the tidepool might be explained by tidally entrained rhythms of gaping behavior that persist from the developmental environment, by tidally driven cues (such as changes in water temperature or food concentration as waves wash into the tidepool at high tide) or from endogenous rhythms. The spectral analyses provide evidence for the latter of these three hypotheses, given the secondary peak at 24 h period in the tidepool and low shore sites, as opposed to the full tidal period of 24 h 50 m at the high shore site. As we discuss below, developmental environment also appears to have long-lasting impacts on mussels' behavior.

Spectral analysis of valve gaping patterns did not reveal any evidence of short-term rhythmic opening and closing of the valves while mussels were submerged. Qualitative examination of individual mussels' gape time series bears this out as well, with individual mussels occasionally closing the valves briefly for a few minutes during a submergence period, perhaps because of occasional disturbances by large waves or predators (Dowd and Somero, 2013; Robson et al., 2010), but not following any obvious rhythmic pattern of opening and closing. The similarity between low shore and constantly submerged tidepool mussels may indicate that desiccation stress and temperature stress are not necessarily the predominant drivers of valve closure in these situations.

Although some species of rocky intertidal bivalves are known to electively gape and potentially use evaporative cooling to avoid high temperatures (Lathlean et al., 2016; Nicastro et al., 2012), we found no evidence that *M. californianus* used a gaping strategy on the warmest low tides, similar to findings from prior studies in the field and laboratory (Bayne et al., 1976b; Fitzhenry et al., 2004). As a group, the *M. californianus* in our experiment generally kept valve gape openings between 0 and 12.2% during hot periods (body temperatures above 25°C), with a median opening of 1.4%, which should reflect a gap between shell valves of less than 100 µm for this size of mussel. This would be sufficient to only expose a small fraction of the mantle edge to the air, where evaporation would be limited by the rate of free water loss from the mantle surface and likely by a low vapor pressure deficit in the boundary layer of moist air in the mussel bed (Helmuth, 1998; Jost and Helmuth, 2007). Although the shift from no evaporation in a fully closed mussel to

the small amount of evaporation possible from a small gape opening might influence body temperature, the strong correspondence in maximum temperatures, heating rates and ranges in maximum temperature among live mussels and silicone-filled mussel mimics at the high shore site indicates that *M. californianus* were likely not using evaporative cooling via valve gaping as a means to control their body temperature in warm low tide conditions.

Persistent effects of developmental environment on gaping behavior

The mussels used in this experiment had originally settled and spent several years growing in either a wave-protected or a wave-exposed location at similar shore heights at HMS. Our assumption, based on previous documentation of these origin sites (Denny et al., 2011; Dowd et al., 2013), was that mussels settling and growing in the wave-exposed location had likely spent less time being thermally stressed at low tide and had more time available to feed while submerged by waves. Mussels at the wave-protected site would have been exposed to a greater number of prolonged aerial emersions and warmer temperatures, which likely required them to be more tolerant of desiccation and temperature stress. When we placed mussels from both origin sites at our three experimental sites, the mussels originally from the wave-protected site gaped more widely on average than their immediate neighbors from the wave-exposed site living on the same experimental plate, when considering all phases of the tidal cycle. This difference in gape distributions, although small, may reflect the wave-protected mussels' willingness to leave their valves open longer during high tide and the falling low tide, increasing the time available to aerobically respire and feed. Whether these behavioral differences reflect genetic variation among sites or developmental fixation of behavior represents an intriguing line of future study.

Impacts of more recent environmental experience were superimposed on these putative developmental effects on behavior. Higher offshore wave heights increased the time spent gaping during a high tide. Larger waves should submerge mussels sooner on a rising tide and leave them splashed longer on the subsequent falling tide. Contrary to our expectations based on stress-related hypotheses, warmer body temperatures during the prior low tide were not strongly correlated with time spent gaping at high tide. However, the hottest body temperatures were also often experienced on days with the smallest waves, restricting the amount of time around high tide when the mussels would be splashed. Consequently, body temperature had a smaller effect on time spent gaping during the subsequent high tide compared with the effect of increasing wave heights. Notably, there was also a significant interaction between prior maximum body temperature and mussel origin, with mussels from the wave-exposed site showing a smaller decrease in time spent gaping as low tide temperatures rose compared with the protected-origin mussels.

Little evidence for directional orientation changes

Our experimental mussels were originally allowed to attach to the experimental plates in a variety of orientations based on where the sensor leads were routed and how neighboring mussels attached themselves. With the caveat that individual mussel movement might be somewhat restricted by the additional pull of the sensor leads, we did not see evidence of mussels (whether instrumented or not) adopting one consistent orientation by the end of this field deployment. Qualitatively, much of the change in orientation between consecutive low tide periods appears more consistent with chance variation in how a mussel came to rest on its tether of byssal threads after being jostled by waves during the intervening high tide, rather than a coherent pattern resulting from active deposition and release of byssal threads to achieve a 'desired' orientation. Thus, while tide-to-tide changes in orientation were 7 deg on average, the cumulative change of mussels' orientation across 43 low tide periods in the dataset only averaged 30 deg, because many of the short-term shifts registered at one low tide were likely countered by a stochastic reversal during a subsequent low tide. Consistent with this conjecture, the mussels on the tidepool plate moved the least between subsequent low tide periods. These tidepool mussels were much less likely to experience intense wave impact forces than those on the intertidal plates (O'Donnell and Denny, 2008). The limited movement of these adult *M. californianus* is consistent with work showing that adult *M. edulis* and *M. galloprovincialis* move little once established in beds (Schneider et al., 2005). Adjusting body posture by releasing and re-secreting protein-rich byssal threads is an energetically expensive venture, and our results suggest that the risk of being washed away by waves if attachment is weak (Carrington, 2002; Moeser et al., 2006) outweighs any potential advantage of adjusting orientation to the sun to minimize solar heating.

Conclusions

Our work with live mussels confirms prior observations from mussel mimics that individual *M. californianus* located only a few body lengths apart within the same single-layer mussel bed can experience very different temperature conditions (Denny et al., 2011; Jimenez et al., 2015). Unlike lizards and other motile species (e.g. Muth, 1977), this persistent inter-individual variation in body temperature appears unmodified by valve-gaping behavior or postural adjustments. The seeming reluctance of *M. californianus* to gape the valves even during high temperature exposures during low tide removes the ability to reduce body temperatures via evaporative cooling. There was little change in body orientation of mussels over the 3 weeks of this study, suggesting that mussels were not attempting to reorient the body to minimize solar heat gain. These data also indicate a surprising amount of variation among mussels in time spent gaping during immersion, particularly at the low shore and tidepool sites. There was relatively little variation in time spent gaping among mussels at the high shore site, presumably because emersion time owing to the tides is an overwhelming driver of behavior at this site. The need to feed and to aerobically respire during the limited submersion time of high tide, combined with the need to avoid desiccation during aerial emersion at low tide, constrains variation in gaping behavior among mussels in a high shore bed. To our surprise, the data provide evidence for persistent effects of developmental environment on gaping behavior, even when mussels are transplanted to sites with different wave-exposure and temperature regimes. The combination of variation in body temperature and behavior can produce very different physiological profiles for mussels growing in the same bed, which could manifest as large variations in stress, energetic demands, growth rates and survival among neighbors. These potential consequences of small-scale variation likely complicate predictions of biological responses to environmental change.

APPENDIX

Body temperature

Variation in daily maxima and minima among sites and individuals

Using the subset of six to seven mussels per plate that had functional temperature sensors for the entire deployment (21 full days), average daily minimum temperatures were significantly lower at the high site relative to the other locations ($F_{2,18}$=33.09, P<0.001; Tukey's HSD

P<0.001 for high versus low and high versus tidepool), though the absolute difference between minimum temperatures averaged less than 1.3°C (Fig. 2A). The average daily temperatures among the three plates were significantly different ($F_{2,18}$=19.99, P<0.001) because of the warmer temperatures achieved at the high shore site (Tukey's HSD, P<0.001 for high versus low and high versus tidepool, no difference for low versus tidepool), although the absolute difference in daily average temperature was no more than 1.2°C (Fig. 2B). The average daily maximum temperatures for mussels were significantly higher at the high shore site ($F_{2,18}$=42.9, P<0.001) compared with the low shore and tidepool sites (Tukey's HSD, P<0.001 for high versus low and high versus tidepool, no significant difference between low and tidepool sites, P=0.216; Fig. 2C).

Inter-individual variation in heating and cooling rates

Summary statistics for the analysis of heating and cooling rates are given in Table 2. The fastest rate of heating observed during the experiment occurred on the high shore plate (Q^{+}_{max}=20.2°C h^{-1}), and the high shore plate also showed the greatest mean range and maximum range in heating rates among mussels on the same plate (5.4 and 14.7°C h^{-1}, respectively). The low shore plate had a maximum heating rate of 12.4°C h^{-1} and a smaller mean range of heating rates (1.8°C h^{-1}). Across all days of the deployment, the average rate of heating for individuals on the high plate was more than twice as fast as mussels on the low shore and tidepool plates (6.79°C h^{-1} for the high shore plate versus ≤1.32°C h^{-1} for the others). The mean $CV_{Q^{+}_{max}}$ was relatively small on the high shore and tidepool plates (0.26 and 0.27, respectively) relative to the low shore plate (0.42). The high shore plate exhibited a consistently larger range of heating rates compared with the tidepool plate, but both plates were relatively consistent in their heating rate CV across the days of the experiment, compared with the low shore plate.

Maximal cooling rates were similar for the high shore and low shore plates (Q^{-}_{max}=–22.8 and –16.8°C h^{-1}, respectively), while the tidepool plate had a much lower maximal cooling rate of −5.3°C h^{-1}, reflecting the smaller range of temperatures experienced in the tidepool owing to the thermal buffering of the water, which was also reflected in the smaller mean and s.d. of the range of Q^{-}_{max} in the tidepool. The low shore plate had the largest mean $CV_{Q^{-}_{max}}$ (−0.47), again owing to a few individual mussels higher on the plate experiencing much warmer temperatures on a subset of days.

Acknowledgements

We thank the faculty and staff of HMS, particularly Mark Denny, for hosting us during our summer field season. Shaina Alves assisted with the collection and deployment of the mussels. Henry Jordan and Andrew Petersen helped develop a prototype on which the MusselTracker system was based.

Competing interests

The authors declare no competing or financial interests.

Author contributions

Conceptualization: W.W.D.; Methodology: L.P.M., W.W.D.; Software: L.P.M.; Investigation: L.P.M., W.W.D.; Data curation: L.P.M.; Writing - original draft: L.P.M., W.W.D.; Visualization: L.P.M.; Funding acquisition: W.W.D.

Funding

This work was supported by National Science Foundation IOS grant 1256186 to W.W.D.

Data availability

Data and associated analysis code are available from the Dryad Digital Repository (Miller and Dowd, 2017): https://doi.org/10.5061/dryad.2sd19. MusselTracker hardware designs and software are available at https://github.com/millerlp/MusselTracker and https://github.com/millerlp/MusselTrackerlib.

Supplementary information

Supplementary information available online at http://jeb.biologists.org/lookup/doi/10.1242/jeb.164020.supplemental

References

Angilletta, M. J. (2009). *Thermal Adaptation: A Theoretical and Empirical Synthesis*. Oxford: Oxford University Press.

Ballesta-Artero, I., Witbaard, R., Carroll, M. L. and van der Meer, J. (2017). Environmental factors regulating gaping activity of the bivalve *Arctica islandica* in Northern Norway. *Mar. Biol.* **164**, 116.

Barnes, G. E. (1955). The behaviour of *Anodonta cygnea* L., and its neurophysiological basis. *J. Exp. Biol.* **32**, 158-174.

Bayne, B. L., Bayne, C. J., Carefoot, T. C. and Thompson, R. J. (1976a). The physiological ecology of *Mytilus californianus* Conrad. I. Metabolism and energy balance. *Oecologia* **22**, 211-228.

Bayne, B. L., Bayne, C. J., Carefoot, T. C. and Thompson, R. J. (1976b). The physiological ecology of *Mytilus californianus* Conrad. II. Adaptations to low oxygen tension and air exposure. *Oecologia* **22**, 229-250.

Bertness, M. D. and Grosholz, E. (1985). Population dynamics of the ribbed mussel, *Geukensia demissa*: the costs and benefits of an aggregated distribution. *Oecologia* **67**, 192-204.

Buckley, B. A., Owen, M.-E. and Hofmann, G. E. (2001). Adjusting the thermostat: the threshold induction temperature for the heat-shock response in intertidal mussels (genus *Mytilus*) changes as a function of thermal history. *J. Exp. Biol.* **204**, 3571-3579.

Byrne, R. A., Gnaiger, E., McMahon, R. F. and Dietz, T. H. (1990). Behavioral and metabolic responses to emersion and subsequent reimmersion in the freshwater bivalve, *Corbicula fluminea*. *Biol. Bull.* **178**, 251-259.

Carrington, E. (2002). The ecomechanics of mussel attachment: from molecules to ecosystems. *Integr. Comp. Biol.* **42**, 846-852.

Carrington, E., Moeser, G. M., Thompson, S. B., Coutts, L. C. and Craig, C. A. (2008). Mussel attachment on rocky shores: the effect of flow on byssus production. *Integr. Comp. Biol.* **48**, 801-807.

Chapperon, C. and Seuront, L. (2011). Space-time variability in environmental thermal properties and snail thermoregulatory behaviour. *Funct. Ecol.* **25**, 1040-1050.

Dayton, P. K. (1971). Competition, disturbance, and community organization: the provision and subsequent utilization of space in a rocky intertidal community. *Ecol. Monogr.* **41**, 351-389.

Dayton, P. K. (1972). Toward an understanding of community resilience and the potential effects of enrichments to the benthos at McMurdo Sound, Antarctica. In *Proceedings of the Colloquium on Conservation Problems in Antarctica* (ed. B. C. Parker), pp. 81-96. Allen Press.

de Paoli, H., van der Heide, T., van den Berg, A., Silliman, B. R., Herman, P. M. J. and van de Koppel, J. (2017). Behavioral self-organization underlies the resilience of a coastal ecosystem. *Proc. Natl Acad. Sci. USA* **114**, 8035-8040.

Denny, M. W. (1995). Predicting physical disturbance: mechanistic approaches to the study of survivorship on wave-swept shores. *Ecol. Monogr.* **65**, 371-418.

Denny, M. W., Hunt, L. J. H., Miller, L. P. and Harley, C. D. G. (2009). On the prediction of extreme ecological events. *Ecol. Monogr.* **79**, 397-421.

Denny, M. W., Dowd, W. W., Bilir, L. and Mach, K. J. (2011). Spreading the risk: Small-scale body temperature variation among intertidal organisms and its implications for species persistence. *J. Exp. Mar. Biol. Ecol.* **400**, 175-190.

Diggle, P. J. (1990). *Time Series: A Biostatistical Introduction*. Oxford: Oxford University Press.

Dong, Y., Miller, L. P., Sanders, J. G. and Somero, G. N. (2008). Heat-shock protein 70 (Hsp70) expression in four limpets of the genus *Lottia*: interspecific variation in constitutive and inducible synthesis correlates with *in situ* exposure to heat stress. *Biol. Bull.* **215**, 173-181.

Dowd, W. W. and Somero, G. N. (2013). Behavior and survival of *Mytilus* congeners following episodes of elevated body temperature in air and seawater. *J. Exp. Biol.* **216**, 502-514.

Dowd, W. W., Felton, C. A., Heymann, H. M., Kost, L. E. and Somero, G. N. (2013). Food availability, more than body temperature, drives correlated shifts in ATP-generating and antioxidant enzyme capacities in a population of intertidal mussels (*Mytilus californianus*). *J. Exp. Mar. Biol. Ecol.* **449**, 171-185.

Fitzhenry, T., Halpin, P. M. and Helmuth, B. (2004). Testing the effects of wave exposure, site, and behavior on intertidal mussel body temperatures: applications and limits of temperature logger design. *Mar. Biol.* **145**, 339-349.

García-March, J. R., Sanchís Solsona, M. Á. and García-Carrascosa, A. M. (2008). Shell gaping behaviour of *Pinna nobilis* L., 1758: circadian and circalunar rhythms revealed by in situ monitoring. *Mar. Biol.* **153**, 689-698.

García-March, J. R., Jiménez, S., Sanchis, M. A., Monleon, S., Lees, J., Surge, D. and Tena-Medialdea, J. (2016). In situ biomonitoring shows seasonal patterns and environmentally mediated gaping activity in the bivalve, *Pinna nobilis*. *Mar. Biol.* **163**, 29.

Gleason, L. U., Miller, L. P., Winnikoff, J. R., Somero, G. N., Yancey, P. H., Bratz, D., Dowd, W. W. (2017). Thermal history and gape of individual *Mytilus*

californianus correlate with oxidative damage and thermoprotective osmolytes. *J. Exp. Biol.* **220**, 4292-4304.
Harger, J. R. E. (1968). The role of behavioral traits in influencing the distribution of two species of sea mussel, *Mytilus edulis* and *Mytilus californianus*. *Veliger* **11**, 45-49.
Harley, C. D. G. (2008). Tidal dynamics, topographic orientation, and temperature-mediated mass mortalities on rocky shores. *Mar. Ecol. Prog. Ser.* **371**, 37-46.
Harley, C. D. G. (2011). Climate change, keystone predation, and biodiversity loss. *Science* **334**, 1124-1127.
Harley, C. D. G. and Helmuth, B. S. T. (2003). Local- and regional-scale effects of wave exposure, thermal stress, and absolute versus effective shore level on patterns of intertidal zonation. *Limnol. Oceanogr.* **48**, 1498-1508.
Hayford, H. A., Gilman, S. E. and Carrington, E. (2015). Foraging behavior minimizes heat exposure in a complex thermal landscape. *Mar. Ecol. Prog. Ser.* **518**, 165-175.
Helmuth, B. S. T. (1998). Intertidal mussel microclimates: predicting the body temperature of a sessile invertebrate. *Ecol. Monogr.* **68**, 51-74.
Helmuth, B. and Denny, M. W. (2003). Predicting wave exposure in the rocky intertidal zone: do bigger waves always lead to larger forces? *Limnol. Oceanogr.* **48**, 1338-1345.
Helmuth, B. S. T. and Hofmann, G. E. (2001). Microhabitats, thermal heterogeneity, and patterns of physiological stress in the rocky intertidal zone. *Biol. Bull.* **201**, 374-384.
Helmuth, B., Harley, C. D. G., Halpin, P. M., O'Donnell, M., Hofmann, G. E. and Blanchette, C. A. (2002). Climate change and latitudinal patterns of intertidal thermal stress. *Science* **298**, 1015-1017.
Helmuth, B., Broitman, B. R., Blanchette, C. A., Gilman, S. E., Halpin, P. M., Harley, C. D. G., O'Donnell, M. J., Hofmann, G. E., Menge, B. A. and Strickland, D. (2006). Mosaic patterns of thermal stress in the rocky intertidal zone: implications for climate change. *Ecol. Monogr.* **76**, 461-479.
Helmuth, B., Choi, F., Matzelle, A., Torossian, J. L., Morello, S. L., Mislan, K. A. S., Yamane, L., Strickland, D., Szathmary, P. L., Gilman, S. E. et al. (2016). Long-term, high frequency in situ measurements of intertidal mussel bed temperatures using biomimetic sensors. *Sci. Data* **3**, 160087.
Huey, R. B. Tewksbury, J. J. (2009). Can behavior douse the fire of climate warming? *Proc. Natl. Acad. Sci. USA* **106**, 3647-3648.
Huey, R. B., Peterson, C. R., Arnold, S. J. and Porter, W. P. (1989). Hot rocks and not-so-hot rocks: retreat-site selection by garter snakes and its thermal consequences. *Ecology* **70**, 931-944.
Jimenez, A. G., Jayawardene, S., Alves, S., Dallmer, J. and Dowd, W. W. (2015). Micro-scale environmental variation amplifies physiological variation among individual mussels. *Proc. R. Soc. B* **282**, 20152273.
Jost, J. and Helmuth, B. (2007). Morphological and ecological determinants of body temperatures of *Geukensia demissa*, the Atlantic ribbed mussel, and their effects on mussel mortality. *Biol. Bull.* **213**, 141-151.
Jou, L.-J., Lin, S.-C., Chen, B.-C., Chen, W.-Y. and Liao, C.-M. (2013). Synthesis and measurement of valve activities by an improved online clam-based behavioral monitoring system. *Comput. Electron. Agric.* **90**, 106-118.
Kearney, M., Shine, R. and Porter, W. P. (2009). The potential for behavioral thermoregulation to buffer "cold-blooded" animals against climate warming. *Proc. Natl. Acad. Sci. USA* **106**, 3835-3840.
Lathlean, J. A., Seuront, L., McQuaid, C. D., Ng, T. P. T., Zardi, G. I. and Nicastro, K. R. (2016). Cheating the locals: invasive mussels steal and benefit from the cooling effect of indigenous mussels. *PLoS ONE* **11**, e0152556.
Li, Q. and Griffiths, J. G. (2004). Least squares ellipsoid specific fitting. In *Geometric Modeling and Processing, 2004 Proceedings*, pp. 335-340. IEEE.
Lockwood, B. L., Sanders, J. G. and Somero, G. N. (2010). Transcriptomic responses to heat stress in invasive and native blue mussels (genus *Mytilus*): molecular correlates of invasive success. *J. Exp. Biol.* **213**, 3548-3558.
Miller, L. P. and Denny, M. W. (2011). Importance of behavior and morphological traits for controlling body temperature in littorinid snails. *Biol. Bull.* **220**, 209-223.
Miller, L. P. and Dowd, W. W. (2017) Data from: Multimodal *in situ* datalogging quantifies inter-individual variation in thermal experience and persistent origin effects on gaping behavior among intertidal mussels (*Mytilus californianus*). Dryad Digital Repository. https://doi.org/10.5061/dryad.2sd19
Miller, L. P., Harley, C. D. G. and Denny, M. W. (2009). The role of temperature and desiccation stress in limiting the local-scale distribution of the owl limpet, *Lottia gigantea*. *Funct. Ecol.* **23**, 756-767.
Moeser, G. M., Leba, H. and Carrington, E. (2006). Seasonal influence of wave action on thread production in *Mytilus edulis*. *J. Exp. Biol.* **209**, 881-890.
Muth, A. (1977). Body temperatures and associated postures of the zebra-tailed lizard, *Callisaurus draconoides*. *Copeia* **1977**, 122-125.
Nicastro, K. R., Zardi, G. I., McQuaid, C. D., Pearson, G. A. and Serrão, E. A. (2012). Love thy neighbour: group properties of gaping behaviour in mussel aggregations. *PLoS ONE* **7**, e47382.
O'Donnell, M. J. (2008). Reduction of wave forces within bare patches in mussel beds. *Mar. Ecol. Prog. Ser.* **362**, 157-167.
O'Donnell, M. J. and Denny, M. W. (2008). Hydrodynamic forces and surface topography: centimeter-scale spatial variation in wave forces. *Limnol. Oceanogr.* **53**, 579-588.
Ozyagcilar, T. (2012). Implementing a tilt-compensated eCompass using accelerometer and magnetometer sensors. Freescale Semiconductor. https://cache.freescale.com/files/sensors/doc/app_note/AN4248.pdf.
Paine, R. T. (1974). Intertidal community structure: experimental studies on the relationship between a dominant competitor and its principal predator. *Oecologia* **15**, 93-120.
Petes, L. E., Menge, B. A. and Murphy, G. D. (2007). Environmental stress decreases survival, growth, and reproduction in New Zealand mussels. *J. Exp. Mar. Biol. Ecol.* **351**, 83-91.
Pincebourde, S., Sanford, E. and Helmuth, B. (2009). An intertidal sea star adjusts thermal inertia to avoid extreme body temperatures. *Am. Nat.* **174**, 890-897.
Pincebourde, S., Sanford, E., Casas, J. and Helmuth, B. (2012). Temporal coincidence of environmental stress events modulates predation rates. *Ecol. Lett.* **15**, 680-688.
Pincebourde, S., Murdock, C. C., Vickers, M. and Sears, M. W. (2016). Fine-scale microclimatic variation can shape the responses of organisms to global change in both natural and urban environments. *Integr. Comp. Biol.* **56**, 45-61.
Pinheiro, J. C. and Bates, D. M. (2000). *Mixed-effects Models in S and S-PLUS*. New York: Springer Verlag.
R Core Team (2016). *R: A Language and Environment for Statistical Computing*. Vienna, Austria: R Foundation for Statistical Computing.
Riisgård, H. U., Lassen, J. and Kittner, C. (2006). Valve-gape response times in mussels (*Mytilus edulis*) – effects of laboratory preceding-feeding conditions and in situ tidally induced variation in phytoplankton biomass. *J. Shellfish Res.* **25**, 901-911.
Robles, C. D., Desharnais, R. A., Garza, C., Donahue, M. J. and Martinez, C. A. (2009). Complex equilibria in the maintenance of boundaries: experiments with mussel beds. *Ecology* **90**, 985-995.
Robson, A. A., Garcia De Leaniz, C., Wilson, R. P. and Halsey, L. G. (2010). Behavioural adaptations of mussels to varying levels of food availability and predation risk. *J. Molluscan Stud.* **76**, 348-353.
Schneider, K. R., Wethey, D. S., Helmuth, B. S. T. and Hilbish, T. J. (2005). Implications of movement behavior on mussel dislodgement: exogenous selection in a *Mytilus* spp. hybrid zone. *Mar. Biol.* **146**, 333-343.
Schwartzmann, C., Durrieu, G., Sow, M., Ciret, P., Lazareth, C. E. and Massabuau, J.-C. (2011). In situ giant clam growth rate behavior in relation to temperature: a one-year coupled study of high-frequency noninvasive valvometry and sclerochronology. *Limnol. Oceanogr.* **56**, 1940-1951.
Shick, J. M., Gnaiger, E., Widdows, J., Bayne, B. L. and De Zwaan, A. (1986). Activity and metabolism in the mussel *Mytilus edulis* L. during intertidal hypoxia and aerobic recovery. *Physiol. Zool.* **59**, 627-642.
Shick, J. M., Widdows, J. and Gnaiger, E. (1988). Calorimetric studies of behavior, metabolism and energetics of sessile intertidal animals. *Am. Zool.* **28**, 161-181.
Shumway, S. E. and Cucci, T. L. (1987). The effects of the toxic dinoflagellate *Protogonyaulax tamarensis* on the feeding and behaviour of bivalve molluscs. *Aquat. Toxicol.* **10**, 9-27.
Shumway, R. H. and Stoffer, D. S. (2011). *Time Series Analysis and Its Applications*. New York: Springer.
Somero, G. N. (2010). The physiology of climate change: how potentials for acclimatization and genetic adaptation will determine 'winners' and 'losers'. *J. Exp. Biol.* **213**, 912-920.
Sow, M., Durrieu, G., Briollais, L., Ciret, P. and Massabuau, J.-C. (2011). Water quality assessment by means of HFNI valvometry and high-frequency data modeling. *Environ. Monit. Assess.* **182**, 155-170.
Stoffer, D. (2016). astsa: Applied Statistical Time Series Analysis. R package version 1.6. https://CRAN.R-project.org/package=astsa.
Suchanek, T. H. (1978). The ecology of *Mytilus edulis* L. in exposed rocky intertidal communities. *J. Exp. Mar. Biol. Ecol.* **31**, 105-120.
Suchanek, T. H. (1979). The *Mytilus californianus* community: studies on the composition, structure, organization, and dynamics of a mussel bed. PhD dissertation, *Department of Zoology*, University of Washington, Seattle, WA.
Suchanek, T. H. (1981). The role of disturbance in the evolution of life history strategies in the intertidal mussels *Mytilus edulis* and *Mytilus californianus*. *Oecologia* **50**, 143-152.
Tran, D., Ciret, P., Ciutat, A., Durrieu, G. and Massabuau, J.-C. (2003). Estimation of potential and limits of bivalve closure response to detect contaminants: application to cadmium. *Environ. Toxicol. Chem.* **22**, 914-920.
Tsuchiya, M. (1983). Mass mortality in a population of the mussel *Mytilus edulis* L. caused by high temperature on rocky shores. *J. Exp. Mar. Biol. Ecol.* **66**, 101-111.